Integrated optical measurement system for fluorescence spectroscopy in microfluidic channels

Hübner, Jörg; Mogensen, Klaus Bo; Jørgensen, Anders Michael; Friis, Peter; Telleman, Pieter; Kutter, Jörg Peter

Published in:
Review of Scientific Instruments

Link to article, DOI:
10.1063/1.1326929

Publication date:
2001

Document Version
Publisher's PDF, also known as Version of record

Integrated optical measurement system for fluorescence spectroscopy in microfluidic channels

Jörg Hübner[a)]
Research Center COM, Ørsteds Plads, Building 345 West, Technical University of Denmark, DK-2800 Lyngby, Denmark

Klaus B. Mogensen, Anders M. Jorgensen, Peter Friis, Pieter Telleman, and Jörg P. Kutter
Mikroelektronik Centret, Ørsteds Plads, Building 345 East, Technical University of Denmark, DK-2800 Lyngby, Denmark

(Received 6 July 2000; accepted for publication 26 September 2000)

A transportable miniaturized fiber-pigtailed measurement system is presented which allows quantitative fluorescence detection in microliquid handling systems. The microliquid handling chips are made in silica on silicon technology and the optical functionality is monolithically integrated with the microfluidic channel system. This results in inherent stability and photolithographic alignment precision. Permanently attached optical fibers provide a rugged connection to the light source, detection, and data processing unit, which potentially allows field use of such systems. Fluorescence measurements with two dyes, fluorescein, and Bodipy 650/665 X, showed good linear behavior over a wide range of concentrations. Minimally detected concentrations were 250 pM for fluorescein and 100 nM for Bodipy. © *2001 American Institute of Physics.*
[DOI: 10.1063/1.1326929]

I. INTRODUCTION

Recently a lot of research effort is directed towards so-called lab-on-a-chip or micrototal analysis systems (μ-TAS). These systems are miniaturized devices where all necessary parts and methods to perform a certain chemical analysis are integrated.[1,2]

A number of analytical procedures have been realized and demonstrated in miniaturized devices, ranging from various sample pretreatment techniques[3–5] to separation and reaction systems involving sophisticated handling of tiny amounts of liquids.[6–8] Targeted applications of such μ-TAS are ranging from point-of-care diagnostics and high throughput screening to environmental monitoring, tools for forensics and food quality control.[9,10] A crucial component for almost any miniaturized analytical device is the detection unit. Among the possible detection methods and principles, which can be integrated, optical detection is the most common tool in modern chemical and biochemical analysis. In particular, fluorescence detection proves to be superior with respect to sensitivity and obtainable limits of detection. Fluorescent marker molecules can be chemically attached to a specific sample molecule of interest so that fluorescence spectroscopy can be used for quantitative analysis. Traditionally, this approach includes bulk optic equipment such as lenses and microscope objectives and requires precise mechanical alignment. Integrated optics based on planar waveguides can replace this bulk optic equipment and, at the same time, be fabricated to match the microfluidic channels in size and technology. In our approach, the optics are monolithically integrated with the microfluidic channels. Silica on silicon is used as the technological platform and is very well suited combining the high optical transparency and stability of silica glass with the chemical robustness of this material.[11]

II. TECHNOLOGY

The technology used for monolithic integration of optics and microfluidic systems is based on plasma enhanced chemical vapor deposition, where silica glass is deposited from the gas phase onto a silicon wafer. The system is capable of deposition rates of 160 nm/min for high quality silica glass.

Bulk optical elements are replaced by optical waveguides. To form these waveguides, the silica is deposited in three layers denoted as buffer, core, and cladding layer (see Fig. 1).[12,13] The 12–15 μm thick buffer layer prevents interaction of the light traveling in the core layer with the silicon wafer. On top of the buffer layer, a core layer is deposited. In order to achieve guiding of the light by total internal reflection, the index of the core layer has to be higher than the index of the surrounding buffer and cladding layers. This is achieved by doping the core layer with germanium and nitrogen. The gas mixture for depositing pure silica glass consists of silane (SiH_4) and nitrous oxide (N_2O). By mixing germane (GeH_4) and ammonia (NH_3) to the gas flow, germanosilicaoxynitride is deposited. The amount of incorporated germanium and nitrogen, and thereby the refractive index of the germanosilicaoxynitride, can be controlled by adjusting the respective gas flows into the deposition chamber.[14] The refractive index of the core

[a)]Also at Mikroelektronik Centret, Orsteds Plads, Building 345 East, Technical University of Denmark, DK-2800 Lyngby, Denmark; electronic mail: johu@com.dtu.dk

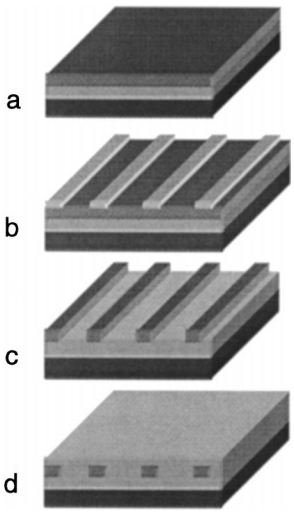

FIG. 1. Sketch of the process sequence to fabricate buried channel waveguides: (a) wafer preparation, buffer growth, and core deposition, (b) photolithography, (c) reactive ion etch, and (d) top cladding deposition.

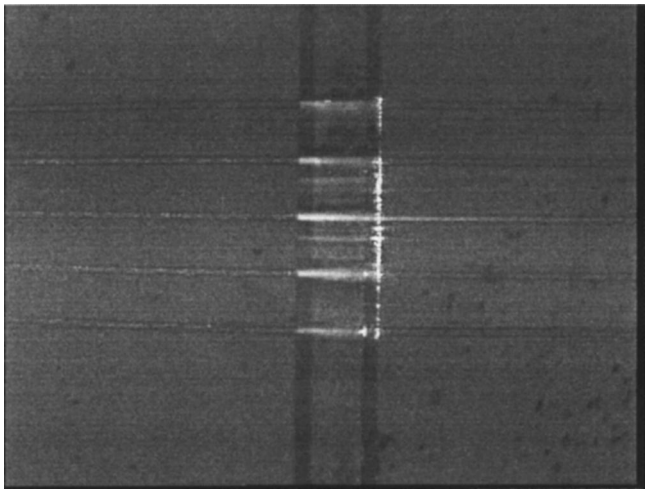

FIG. 2. Visualization of light across a microfluidic channel. Excitation light (488 nm) is split by an integrated Y splitter into five waveguides coupling across a microfluidic channel filled with fluorescein solution. This setup can be used for absorption measurements.

layer is adjusted to be around 1.0%–1.5% higher than the surrounding layers.

The approximately 6 μm thick core layer is subsequently structured using photolithography and reactive ion etching (RIE). The entire structure is then covered by a cladding layer consisting of pure silica glass. After that, the microfluidic channels are etched through the three glass layers into the silicon wafer (according to the desired channel depths), again employing photolithography and RIE. Finally, a thin layer of polysilicon is deposited on the whole structure to enable anodic bonding of a Pyrex® lid covering the entire area of a 4 in. wafer.

III. EXPERIMENTAL SETUP

Test structures, sized around 2 cm by 1 cm, containing a microfluidic channel and several waveguides across this channel were diced out of the 4 in. wafer and polished on both facets perpendicular to the waveguides. To measure the transmission through such a structure, light from a deuterium halogen lamp is coupled into one of the waveguides using an optical fiber. Light traversing the microfluidic channel is collected by the waveguide on the opposite side of the approximately 500 μm broad microfluidic channel (in this particular structure) (see Figs. 2 and 3). An optical fiber collects the light at the end of the waveguide. The connector on the opposite end of that fiber was plugged into an optical spectrum analyzer equipped with a cooled photomultiplier. The optical spectrum analyzer can cover a spectral range reaching from 190 to 1700 nm with a spectral resolution of 0.1 nm. After both fibers are precisely aligned and transmission is maximized, the fibers are permanently attached to the waveguide using UV hardening glue. Transmission spectra of the described configuration reveal that the detection device can be used over a broad wavelength range from 350–1700 nm (see Fig. 3).

For fluorescence spectroscopy, the arrangement of the optical fibers and the geometry are changed in order to avoid collection of excitation light by the waveguide. The excitation light is delivered through the Pyrex® lid using an optical fiber (fiber 1), which is attached to the Pyrex® directly above the microfluidic channel as shown in Fig. 4. The integration of the waveguide allows a 90° angle between excitation and fluorescence collection ensuring that only small amounts of scattered excitation light are collected by the waveguide and reach the detection system via fiber 2. The chosen geometry ensures an efficient separation of excitation and fluorescence light. In the absence of a fluorescent agent, the collected excitation light power in fiber 2 has been measured to be only 190 pW while 870 μW of excitation light was measured out of the excitation fiber (fiber 1). From these numbers, it is calculated that the excitation light is suppressed by more than 60 dB by geometry alone. In addition, a bandpass interference filter centered at 520 nm (± 10 nm) was inserted prior to the detector, thereby reducing the excitation light power below the noise level (see dashed curves in Fig. 5).

Two different lasers were used as light sources. When using fluorescein as reagent, an argon ion laser capable of

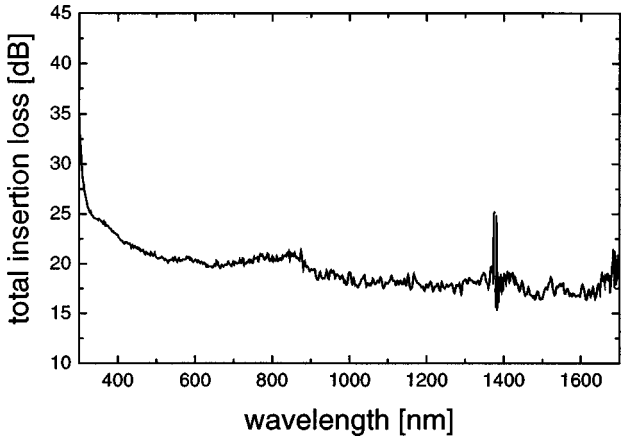

FIG. 3. Transmission spectrum of a structure containing germanosilicaoxynitride waveguides where light is coupled across a microfluidic channel (as shown in Fig. 2 but for a single waveguide without the Y splitter). Spectrum is normalized by a fiber-to-fiber measurement thus indicating the spectrally resolved total insertion loss of the device.

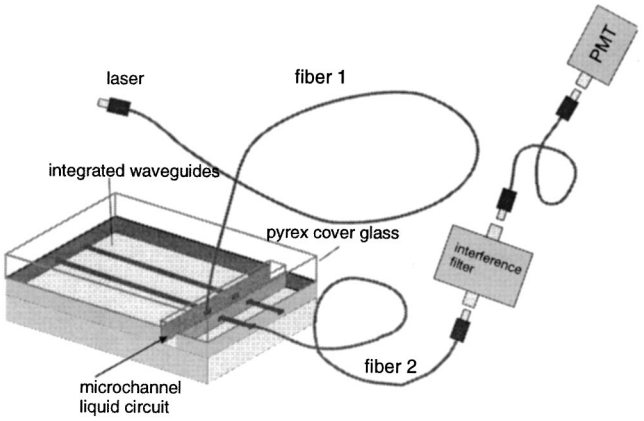

FIG. 4. Schematic view of the fluorescence measurement setup. Excitation light is launched into the microchannel by a single-mode fiber glued on top of the microchannel (fiber 1). Fluorescence light is collected by a fiber terminated (fiber 2) waveguide. Bandpass interference filter further attenuates the excitation light.

delivering around 100 mW at 488 nm was used. Only around 1 mW of power was used for the fluorescence excitation at the end of the excitation fiber, which showed single mode operation at 488 nm. To be able to exploit the advantages of semiconductor lasers (compact, cheap, potentially battery powered), a special dye (Molecular Probes BODIPY 650/665-X, succinimidyl ester) with absorption around 633 nm was used. The semiconductor laser diode was pigtailed with a fiber exhibiting single mode operation around the lasing wavelength of 637 nm and capable of delivering around 4 mW at the end of the excitation fiber. By using a fiber pigtailed laser diode as light source which can easily be battery powered, the whole optical system is permanently attached to fiber optic cables equipped with optical connectors and thereby alignment free, stable, easily transportable, and hence suitable for field use.

In order to have a well-defined illuminated area in the channel the fiber delivering the excitation light is single mode at the respective excitation wavelength. A multimode fiber used for this purpose may introduce mode noise in the illuminated area due to coupling between modes, which may be caused by bends and vibrations of the fiber. An additional advantage of a single mode fiber is its small core size of below 10 μm and hence a small illuminated area where the fluorescent dye is excited with high intensity.

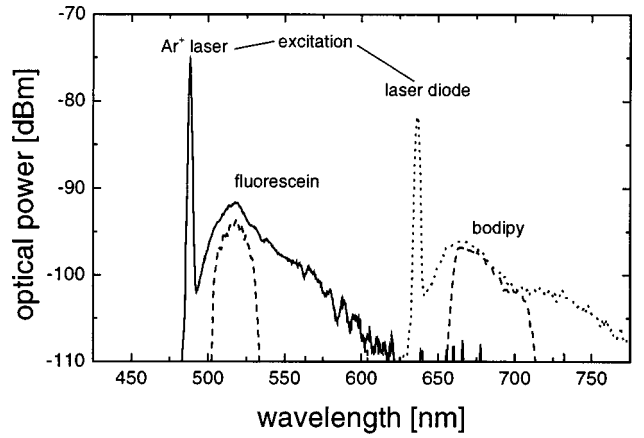

FIG. 5. Fluorescence spectra of two different dyes with (dashed line) and without interference filter. The fluorescence is collected from the microfluidic channel using the configuration shown in Fig. 4. Solid line represents the fluorescence spectrum of a solution of fluorescein in borate buffer with a fluorescein concentration of 1 μm. The dotted curve was taken by injecting a solution of Bodipy 650/665-X, succinimidyl ester in borate buffer. The Bodipy concentration was 52 μM.

IV. RESULTS AND DISCUSSION

Figure 5 shows the excitation and fluorescence spectra of the two different excitation laser/dye combinations. In order to estimate the number of fluorescent molecules needed to detect a certain concentration, the detection volume has to be calculated. This can be done by estimating the part of the illuminated volume from where the fluorescence is collected by the optical waveguide.

To roughly estimate the illuminated volume, the actual spot size in the channel at half the channel depth is calculated using the following formula:

$$A_{\text{spot}} = \pi \left[d_{\text{lid}} \tan\left(\arcsin\left(\frac{\text{NA}_{\text{fib}}}{n_{\text{lid}}} \right) \right) + \frac{d_{\text{channel}}}{2} \tan\left(\arcsin\left(\frac{\text{NA}_{\text{fib}}}{n_{\text{liq}}} \right) \right) \right]^2,$$

where d_{lid} and n_{lid} represent the thickness and refractive index of the Pyrex® lid, respectively, d_{channel} and n_{liq} are the channel depth and the refractive index of the liquid in the channel and NA_{fib} is the numerical aperture of the fiber delivering the excitation light through the Pyrex® lid. The first term represents the beam radius at the lid–liquid interface, while the second term represents the additional increase due to divergence of the beam in the microchannel (refraction at the lid–liquid interface is neglected in the calculation). As the channel depth is around an order of magnitude smaller than the thickness of the Pyrex® lid and the numerical aperture of the fiber NA_{fib} is around 0.12–0.16, it can be assumed that the volume of illuminated liquid in the channel is cylindrical over the channel depth. This leads to an illuminated volume of

$$V_{\text{illu}} \approx A_{\text{spot}} d_{\text{channel}}.$$

In the experiments described, $d_{\text{channel}} = 50\mu\text{m}$, $\text{NA}_{\text{fib}} = 0.16$, $n_{\text{lid}} \approx 1.5$, and $d_{\text{lid}} = 500$ μm and thus the illuminated volume V_{illu} is around 5×10^5 μm^3 or 0.5 nL. The calculated spot radius of around 50 μm shows that this simple geometry leaves room for reduction in the channel width to around 100 μm, which might be advantageous for certain applications.

The detection volume is given by the overlap between the acceptance cone of the waveguide and the illuminated volume in the microchannel. The spot radius of the excitation light in the microfluidic channel as described above is twice the size of the waveguide width. The illuminated volume extends from the waveguide microchannel interface to about 100 μm within the microchannel. The estimated detection volume is thus given by

$$V_{\mathrm{det}} = 1/2 r_{\mathrm{spot}} \left[h_{\mathrm{waveguide}} + 2 r_{\mathrm{spot}} \tan\left(\frac{\sqrt{n_{\mathrm{core}}^2 - n_{\mathrm{clad}}^2}}{n_{\mathrm{liq}}} \right) \right] \times \left[w_{\mathrm{waveguide}} + 2 r_{\mathrm{spot}} \tan\left(\frac{\sqrt{n_{\mathrm{core}}^2 - n_{\mathrm{clad}}^2}}{n_{\mathrm{liq}}} \right) \right],$$

where r_{spot} is the spot radius, $h_{\mathrm{waveguide}}$ is the height of the waveguide, $w_{\mathrm{waveguide}}$ is the waveguide width and n_{core} and n_{clad} are the refractive indices of the core and cladding layer, respectively. The second term in each bracket accounts for the divergence of the beam due to refraction at the waveguide–liquid interface. The detection volume is calculated to approximately 0.1 nL, which corresponds to about 15 000 molecules at a fluorescein concentration of 250 pM.

The spot size calculation shown also allows an estimate on the laser intensity in the microchannel. Although the collected fluorescence power is a monotonous function of the incident excitation light intensity, fluorescence quenching is a serious problem for absolute calibration of the system (fluorescent power is a function of reagent throughput and concentration). The irradiance of the excitation light in the channel is given by the laser power in the fiber divided by the spot size A_{spot}. For the fiber used in our experiment, the spot size is around 10 000 μm^2, which leads to intensities in the order of several tens of watt per square centimeter for excitation light power in the milliwatt range.

The sensitivity of the measurement system is determined by the properties of the guided wave optics and the detector properties. In this article, we concentrate on the guided wave optics, as several suitable detector systems are commercially available. The following results have been obtained using different photomultiplier based detector schemes. Important for field use is the possibility of using a battery-driven photomultiplier module with an integrated amplifier. Such a module was also evaluated and performed very satisfactory.

The optical performance is determined by the overall loss in the light path and the ability of the waveguide to collect the emitted fluorescent light. The overall loss in the optical path is a combination of coupling loss and propagation loss. The propagation loss of the integrated waveguide has been measured to be below 0.5 dB/cm for visible light. With a waveguide length of around 0.5 cm, the propagation loss is estimated to be not more than 0.3 dB. For the fibers, the propagation loss in the visible wavelength range is negligible (of the order of dB/km). The spectral range where the total propagation loss (fiber+waveguide) is below 3 dB extends from around 380 nm to 1700 nm. Coupling losses are, compared to propagation losses, much more severe in these systems. Especially the rectangular shape of the waveguide compared to the round core shape of the optical fiber gives rise to elevated coupling losses. These losses are strongly dependent on the fibers used. Core diameter and numerical aperture of the fiber compared to the waveguide determine the coupling loss. Coupling from the optical waveguide to the fiber is maximized when the respective numerical apertures match and the core of the fiber has the same dimension as the core of the optical waveguide. A standard core size for multimode optical fibers is 50 μm, which was used during the experiments. The waveguides were 4 μm by 24 μm and the core cladding refractive index difference was around 1.2%. The total (fiber to fiber) insertion loss including a 500 μm broad microchannel was measured to be in the order of 18 dB.

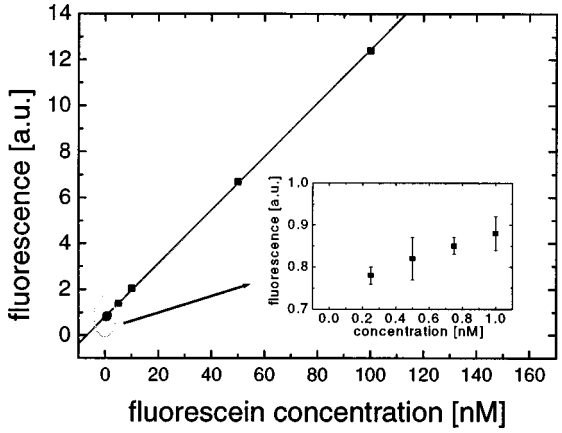

FIG. 6. Dependence of the fluorescence signal on dye concentration for fluorescein. A 488 nm Ar ion laser was used as excitation light source.

Another critical issue determining the sensitivity of the device is the ability of the waveguide to collect fluorescent light in the microfluidic channel. This is mainly determined by the numerical aperture of the waveguide taking into account that this numerical aperture changes with the refractive index of the liquid contained in the channel. The fluorescent measurement unit was developed for chemical or biochemical analysis where a reagent marked with a fluorescent molecule is separated by, e.g., on-chip capillary electrophoresis. To simulate this kind of application, a diluted solution of fluorescent dye was continually pumped through the microfluidic channel and the fluorescent light measured using a photomultiplier based detection unit. In the case of fluorescein diluted in a borate buffer, concentrations as low as 250 pM could still be detected. Figure 6 shows that the measured light signal is proportional to the fluorescein concentration allowing quantitative measurements over several orders of magnitude. The excitation laser power used in this experiment was 870 μW. This leads to an intensity in the channel of around 9 W/cm^2 on a spot size of approximately 10 000 μm^2. Similarly, with the Bodipy dye and the red laser diode, concentrations down to 100 nM Bodipy in borate buffer could easily be detected. The calibration plot (see Fig. 7) displays a good linearity over the investigated concentration range. Although not as sensitive as the system utilizing the argon ion laser and fluorescein, this system is very cost effective. Its low power consumption allows it to be battery driven and potentially enables applications like continuous reagent monitoring in stand-alone solar powered field sensors.

In summary, the realization of a new optical detection setup for micrototal analysis systems based on guided wave optics is presented. Permanently attached fibers, which are terminated by standard connectors potentially enable this compact, rugged system for field use. The optical waveguides are integrated monolithically with the microfluidic channels and are therefore inherently stable and precisely aligned. Light is guided to and from the device using

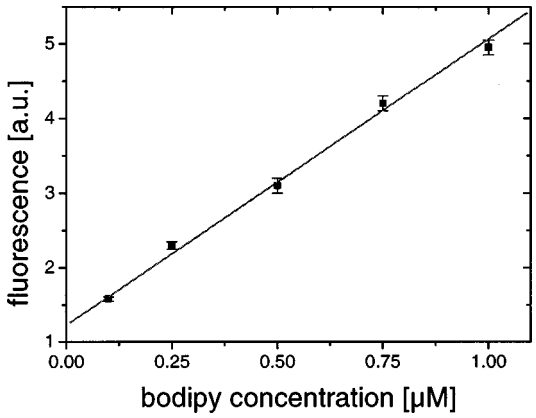

FIG. 7. Dependence of the fluorescence signal on dye concentration for Bodipy. Fiber pigtailed 637 nm semiconductor laser was used as excitation light source.

permanently attached optical fibers. With optical connectors, it is possible to plug the chip to any suitable light source and detection unit working from the near UV range to the far infrared. This ''plug and play'' approach makes this system generally suited for several different chip designs and a variety of possible applications in chemical and biomedical analysis.

[1] A. Manz, N. Graber, and H. M. Widmer, Sens. Actuators B **1**, 244 (1990).
[2] A. van den Berg and T. S. J. Lammerink, *Microsystem Technology in Chemistry and Life Science* (Springer, Berlin, 1998), Vol. 194, pp. 22–49.
[3] L. C. Waters, S. C. Jacobson, N. Kroutchinina, J. Khandurina, R. S. Foote, and J. M. Ramsey, Anal. Chem. **70**, 158 (1998).
[4] J. Cheng, L. J. Kricka, E. L. Sheldon, and P. Wilding, Microsys. Technol. Chem. Life Sci. **194**, 216 (1998).
[5] J. P. Kutter, S. C. Jacobson, and J. M. Ramsey, J. Microcolumn Sep. **12**, 93 (2000).
[6] D. J. Harrison, K. Fluri, K. Seiler, Z. Fan, C. S. Effenhauser, and A. Manz, Science **261**, 895 (1993).
[7] F. E. Regnier, B. He, S. Lin, and J. Busse, Trends Biotechnol. **17**, 101 (1999).
[8] J. P. Kutter, TrAC, Trends Anal. Chem. **19**, 352 (2000).
[9] A. Manz, D. J. Harrison, E. Verpoorte, and H. M. Widmer, *Advances in Chromatography* (Marcel Dekker, New York, 1993), Vol. 33, pp. 1–66.
[10] G. H. W. Sanders and A. Manz, TrAC, Trends Anal. Chem. **19**, 364 (2000).
[11] J. M. Ruano, V. Benoit, J. S. Aitchison, and J. M. Cooper, Anal. Chem. **72**, 1093 (2000).
[12] B. A. M. Andersen, Ph. D. thesis, Technical University of Denmark, 1997.
[13] F. Bruno, M. Del Guidice, R. Recca, and F. Testa, Appl. Opt. **30**, 4560 (1991).
[14] C. V. Poulsen, T. S. Larsen, J. Hübner, and O. Leistiko, Proc. SPIE **2998**, 132 (1997).